Photo-Induced Functionalization of Spherical and Planar Surfaces via Caged Thioaldehyde End-Functional Polymers

*Michael Kaupp, Alexander S. Quick, Cesar Rodriguez-Emmenegger, Alexander Welle, Vanessa Trouillet, Ognen Pop-Georgievski, Martin Wegener, and Christopher Barner-Kowollik**

The synthesis and application of a novel reversible addition-fragmentation chain transfer (RAFT) agent carrying a photocaged thioaldehyde moiety is described (λ_{max} = 355 nm). RAFT polymerization of styrene, dimethylacrylamide and a glycomonomer is evidenced (3600 g mol^{-1} ≤ M_n ≤ 15 000 g mol^{-1}; 1.07 ≤ $Đ$ ≤ 1.20) with excellent end-group fidelity. The photogenerated thioaldehyde on the chain ends can undergo hetero Diels–Alder reactions with dienes as well as reactions with nucleophiles. The terminal photoreactive polymers are photografted to porous diene-reactive polymeric microspheres. The grafted particles are in-depth characterized via scanning electron microscopy, elemental analysis, X-ray photoelectron spectroscopy, and high resolution FT-IR microscopy, leading to a qualitative as well as quantitative image of the core–shell objects. Grafting densities up to 0.10 molecules nm^{-2} are reached. The versatility of the thioaldehyde ligation is evidenced by spatially resolved grafting of polystyrene onto nucleophilic groups present in poly (dopamine) (PDA)-coated glass slides and silicon wafers via two-photon direct laser writing (DLW) imaged by ToF-SIMS. The combination of thioaldehyde ligation, RAFT polymerization, and DLW allows for the spatially resolved grafting of a vast range of polymers onto various substrates in any desired pattern with sub-micrometer resolution.

1. Introduction

There is a strong drive towards the development of novel surface functionalization techniques that require neither tedious pre-functionalizations nor harsh reaction conditions. In addition, spatial control over surface functionalization paves the way to a wide range of applications in research areas including (bio)sensing, biological applications, lab-on-a-chip systems, and microelectronics.[1–5] Harsh conditions as well as the need for catalysts can be circumvented by employing light-induced ligation for covalent surface modifications.

In recent years, a 'tool box' of light-triggered grafting reactions has been developed and employed to graft various (natural and artificial) polymeric structures onto a diverse set of surfaces in a spatially controlled manner. Nitrile imine-mediated tetrazole-ene cycloadditions (NITEC)[6] have been employed to graft polymers onto silicon wafers[7] and cellulose sheets,[8] as well as antifouling brushes onto poly(dopamine) surfaces.[1] However, NITEC typically requires UVC light, which can be harmful when ligating sensitive biomolecules.[9] A second approach introduced by Barner-Kowollik and colleagues is based on the light-induced formation of ortho-quinodimethanes, termed the photo-enol technique.[10] Photo-enols represent highly reactive photocaged dienes for Diels–Alder reactions and can be employed to graft peptides and polymers onto silicon wafers,[11] poly(DOPA) interfaces onto various substrates[12] as well as onto biopolymers such as hyaluronan films and cellulose sheets.[13] A more recent

M. Kaupp, A. S. Quick, Dr. C. Rodriguez-Emmenegger, Dr. A. Welle, Prof. C. Barner-Kowollik
Preparative Macromolecular Chemistry
Institut für Technische Chemie und Polymerchemie
Karlsruhe Institute of Technology (KIT)
Engesserstraße 18, 76128 Karlsruhe, Germany
E-mail: christopher.barner-kowollik@kit.edu

M. Kaupp, A. S. Quick, Dr. C. Rodriguez-Emmenegger, Dr. A. Welle, Prof. C. Barner-Kowollik
Institut für Biologische Grenzflächen
Karlsruhe Institute of Technology (KIT)
Herrmann-von-Helmholtz-Platz 1, 76344
Eggenstein-Leopoldshafen, Germany

DOI: 10.1002/adfm.201400609

A. S. Quick, Prof. M. Wegener
Institut für Angewandte Physik
Institut für Nanotechnologie and Center for Functional Nanostructures
Karlsruhe Institute of Technology (KIT)
Wolfgang-Gaede-Straße 1, 76131 Karlsruhe, Germany

Dr. C. Rodriguez-Emmenegger, Dr. O. Pop-Georgievski
Institute of Macromolecular Chemistry
Academy of Sciences of the Czech Republic v.v.i.
Heyrovsky sq. 2, 162 06 Prague, Czech Republic

V. Trouillet
Institute for Applied Materials (IAM) and Karlsruhe Nano Micro Facility (KNMF)
Karlsruhe Institute of Technology (KIT)
Hermann-von-Helmholtz-Platz 1, 76344
Eggenstein-Leopoldshafen, Germany

strategy is based on the utilization of photogenerated thioaldehydes that can react with nucleophiles and dienes and has successfully been employed to produce polymer patterns on silicone surfaces.[14,15] The ubiquity of nucleophilic groups makes the thioaldehyde approach the most versatile light-induced ligation chemistry, all the more since the applied light (λ_{max} = 355 nm) is the mildest of the aforementioned approaches and, additionally, the photoactive precursor (phenacylthio)acetic acid can be readily synthesized in one facile step from commercially available, low-cost reactants.[16]

All the aforementioned approaches have in common that the surface pattern is achieved by anchoring the photoactive group to the surface. In a subsequent reaction step, the pre-functionalized surface is irradiated through a shadow mask.

Photo-induced grafting reactions can be combined with reversible deactivation radical polymerization (RDRP) techniques such as reversible addition chain transfer (RAFT)[17] polymerization. RAFT is the most versatile RDRP process,[18–21] applicable to more monomer classes than nitroxide-mediated polymerization (NMP)[22] or atom transfer radical polymerization (ATRP),[23,24] while excluding cytotoxic metals and harsh reaction conditions. Minor disadvantages of the RAFT process are the sometimes exhibited deviation from ideal kinetics due to induction periods as well as hybrid behavior and the potential instability of the thiocarbonyl thio groups to some reaction conditions, such as aminolysis.

By attaching the photo-enol precursor group to a RAFT agent, the decoration of polymeric microspheres with various RAFT polymers—including a glycopolymer—was achieved. In addition, a light-triggered approach allowed the synthesis of Janus microspheres.[25] A disadvantage of employing the photo-enol ligation reaction is that residual monomer has to be absent, as the light-generated photo-enol moieties can react with acrylic double bonds.[26]

Cross-linked (porous) polymeric microspheres are a highly interesting substrate for grafting reactions.[27] The entities are facile to synthesize via several techniques, allowing control over properties such as size, porosity and functionality.[28] Microspheres have a wide range of applications from pharmaceuticals[29] and chromatography[30] to organic synthesis.[31] Although variable functionalities can already be incorporated during the microsphere synthesis,[28,32] significant interest lies in grafting polymeric chains onto the particles in order to introduce tailored functionalities and properties.[33–35]

Poly(dopamine) (PDA) films are a bio-inspired polymeric structure from mussel adhesives, which can be formed by spontaneous polymerization of dopamine in aqueous solution.[36,37] PDA can adhere to virtually any surface employing forces ranging from van der Waals to covalent interactions.[38] Surfaces coated with PDA are excellent substrates for cell adhesion.[39,40] PDA has been widely used as an anchor layer of antifouling polymer brushes prepared by 'grafting-to'[38,41,42] and 'grafting-from' methods.[1,37] PDA exhibits amine groups that can be functionalized with moieties enabling thermally induced[43] as well as phototriggered grafting reactions for polymers[1,12] before or after the layer formation.

Direct laser writing (DLW) is a powerful two-photon lithographic technique for the fabrication of various devices on the micrometer scale by employing a highly focused laser beam and a precisely moveable sample sheet.[44–47] Although the main focus of this technique lies in the production of three-dimensional objects, the experimental setup also enables light-induced covalent modification strategies for facile patterning of device surfaces, e.g., via the photo-enol approach.[48] By utilizing light as a reaction trigger, various photochemical reactions can be applied for surface patterning, allowing the spatially resolved covalent attachment of molecules with sub-micrometer resolution. The possibility to alter the wavelength greatly increases the number of potential photochemical systems that can be applied for this process.

The present work combines, for the first time, the light-induced thioaldehyde ligation reaction with RAFT polymerization, thus enabling the photo-induced grafting of any polymer synthesizable by RAFT onto surfaces carrying a nucleophilic motif or diene, such as a carrier material coated with a PDA layer and porous polymeric microspheres. Furthermore, by combination with a DLW setup, any two-dimensional pattern can be grafted onto PDA-coated surfaces with micrometer resolution. In summary, the combination of photo-induced thioaldehyde ligation, RAFT polymerization, and DLW paves the way for tethering a wide variety of polymeric structures to virtually every surface in any micrometer-resolved pattern.

2. Results and Discussion

2.1. Photo-RAFT Agent Design

The design and synthesis of the novel photoreactive RAFT agent containing a phenacyl sulfide follows a similar synthetic rationale to that which we have previously selected for the synthesis of a RAFT agent that carries a photo-enol moiety.[25] It is based on 2-((dodecylsulfanyl)carbonothioyl)sulfanyl propanoic acid (DoPAT), a commonly used trithiocarbonate, which can be readily equipped with a small spacer containing an alcohol function. The alcohol moiety can subsequently be used in a simple Steglich esterification[49] to attach a phenacyl sulfide (**Figure 1**). Under UV-irradiation (λ_{max} = 355 nm), the phenacyl sulfide undergoes photolysis and forms acetophenone and a thioaldehyde, which can react with nucleophiles and dienes (for the UV–vis spectra of DoPATPAS, refer to the Supporting Information, Figure S3).[14–16]

The trithiocarbonate group should be stable under the applied irradiation conditions.[50,51] Nevertheless, to prevent any side reaction leading to degrafting of the photoligated chains, the photoreactive group is attached to the R-group of the RAFT agent. Thus, if any degradation of the Z-group (trithiocarbonate) occurs, the thioaldehyde is still attached to the polymeric chain. The attachment of the photoreactive group to the R-group renders the novel photoreactive RAFT agent thus also suitable for applications demanding harsher reaction conditions, such as intensive UV-light, amines or high temperatures.

2.2. RAFT Polymerization

In order to show that the attachment of the phenacyl sulfide does not influence the ability of the RAFT agent to mediate a

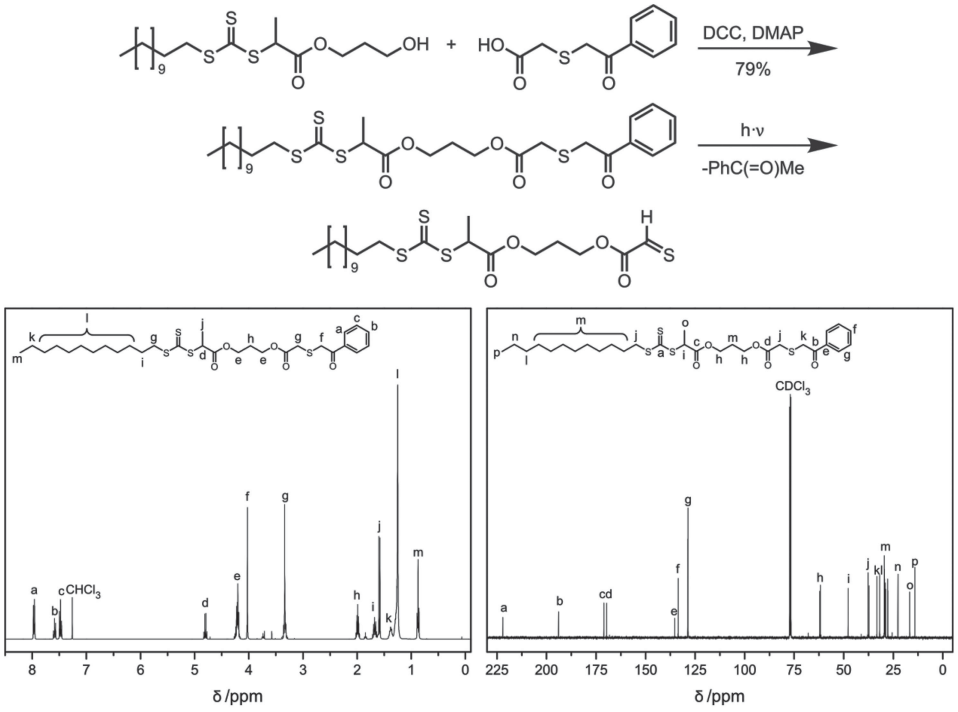

Figure 1. Synthesis and reactivity of the novel photoreactive RAFT agent DoPATPAS; bottom: ^{1}H (left) and ^{13}C (right) NMR spectra.

radical polymerization process, several RAFT polymerizations were conducted utilizing the aforementioned RAFT agent. The versatility and robustness of the approach is demonstrated by choosing rather different and challenging (functional) monomers: styrene, dimethylacrylamide, and a protected glycomonomer 2-(2′,3′,4′,6′-tetra-*O*-acetyl-*β*-D-mannosyloxy)ethylacrylate (AcManEA). The polymerizations were carried out in bulk as well as in solution and were thoroughly analyzed via nuclear magnetic resonance (NMR) spectroscopy, gel permeation chromatography (GPC) and electrospray ionization-mass spectrometry (ESI-MS). The NMR analysis reveal that the resulting polymers still carried both of the RAFT end-groups and can be fully isolated from unreacted monomer (Figure S1, Figure S2, Figure S4). The GPC traces (**Figure 2**) show a monomodal distribution and low dispersities (below 1.1 for polystyrene and PDMAA, 1.2 for PAcManEA, which was polymerized to a higher conversion to achieve a molecular weight that results in a polymer that can be isolated via precipitation). The small shoulder at higher retention times in the case of PAcManEA indicates some termination or transfer side products, which are probably due to the higher conversion which is required to prepare longer chains.

The number average molecular weights derived from GPC and NMR analyses match in the case of polystyrene, yet differ for PDMAA and PAcManEA, where the NMR analysis indicates higher molecular weights. The difference can be readily explained, as all samples were analyzed with the MHKS parameters for styrene (direct calibration), since there are no parameters listed in the literature for the other polymers at the employed conditions.

The analysis via ESI-MS further underlines the controlled behavior of the polymerization, as the spectra show almost exclusively signals which belong to polymeric chains carrying the Z- as well as the R-group of the RAFT agent (**Figure 3**). The structure is indicated by the label P_{RZ} in the spectra, which shows the theoretical mass of a chain containing the intact

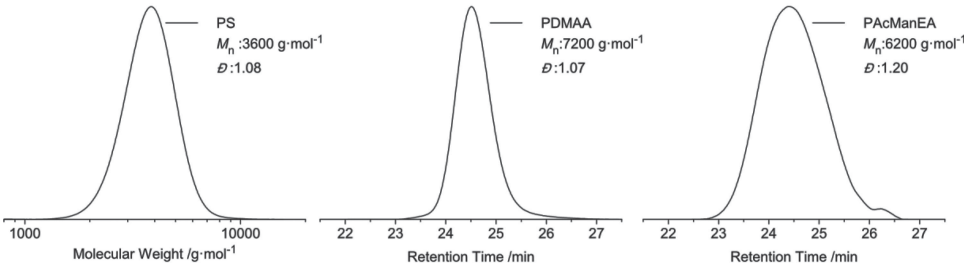

Figure 2. GPC traces of the RAFT polymers synthesized with DoPATPAS. Left: polystyrene in THF; center: PDMAA in DMAc; right: PAcManEA in DMac. All values correspond to linear polystyrene calibration.

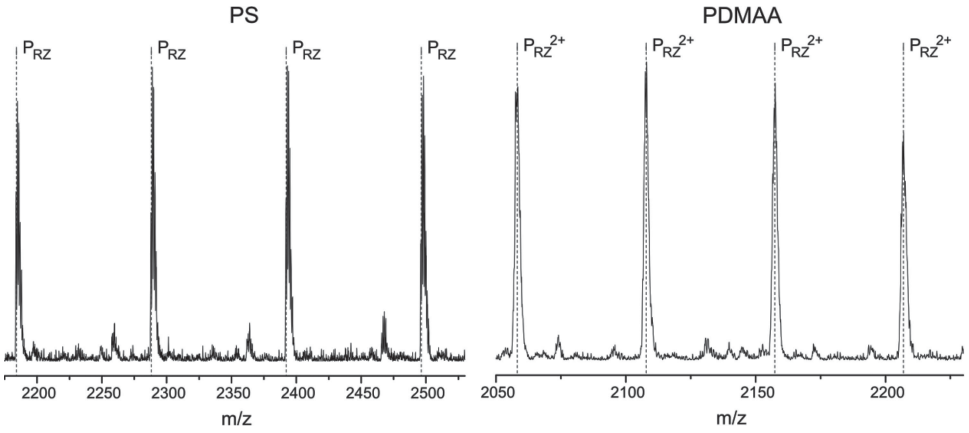

Figure 3. Details from the ESI-MS spectra of polystyrene (left) and poly(*N*,*N*-dimethylacrylamide) (right) polymerized with DoPATPAS. The label P_{RZ} indicates the theoretical mass of chains with the R- and Z-group of the RAFT agent as end-groups, ionized with Na^+ (stemming from added NaTfa).

RAFT agent ionized with a Na^+ ion (lightest isotope for PS, average molecular weight for PDMAA, since for double-charged ions the resolution is too low to show single isotopic peaks in this mass region). The theoretical and experimental *m/z* values match excellently (refer to Table S1 in the Supporting Information).

Since there is a potential bias of the ionization towards higher molecular weights, no information regarding the average molecular weight of the polymer can or should be obtained from mass spectrometric measurements. The relatively high molecular weight of the PAcManEA (M_n = 15 000 g mol^{-1}, derived from NMR) did not allow for an ESI-MS analysis, yet the NMR results (Figure S4) and the low polydispersity also indicate a high end-group functionality.

2.3. Functionalization of Microspheres

2.3.1. Pre-Functionalization, Test, and Control Reaction

Although the photogenerated thioaldehyde can also undergo reactions with a wide range of nucleophiles,[15,16,50] the PGMA microspheres were functionalized with cyclopentadiene moieties, thus employing the released (thioformyl)formate species as a dienophile in a [4+2] cycloaddition. The cycloptentadiene is introduced by employing sodium cyclopentadienide in a single step via a procedure described previously (see the top line of **Figure 4**).[35]

Since the photogenerated thioaldehyde is very reactive, a test experiment was conducted in order to prove that the introduction of the cycloptentadiene strongly increases the rate of the grafting reaction. Thus, two reactions were performed: A grafting reaction between the RAFT agent DoPATPAS and the cyclopentadiene-functionalized microspheres (test reaction), and a grafting reaction between the RAFT agent and the unaltered PGMA microspheres (control reaction) (Figure 4). The amount of microspheres and RAFT agent was identical in both cases (refer to Section 4.5 in the Experimental Section). The reaction was conducted in dichloromethane (DCM) as, due to the similar density of DCM and the spheres, these are evenly dispersed in the solution, leading to an even irradiation of the entire reaction mixture. Subsequently, the suspension was percolated with nitrogen for 20 min and irradiated with a 36 W compact fluorescent lamp (λ_{max} = 355 nm) for 60 min. After thorough filtering, washing, and drying, the spheres were analyzed via scanning electron microscopy (SEM), X-ray photoelectron spectroscopy (XPS) and elemental analysis.

SEM analysis cannot provide any information regarding the chemical changes of the particles, yet it is of critical importance to check if the porosity and spherical shape of the particles is

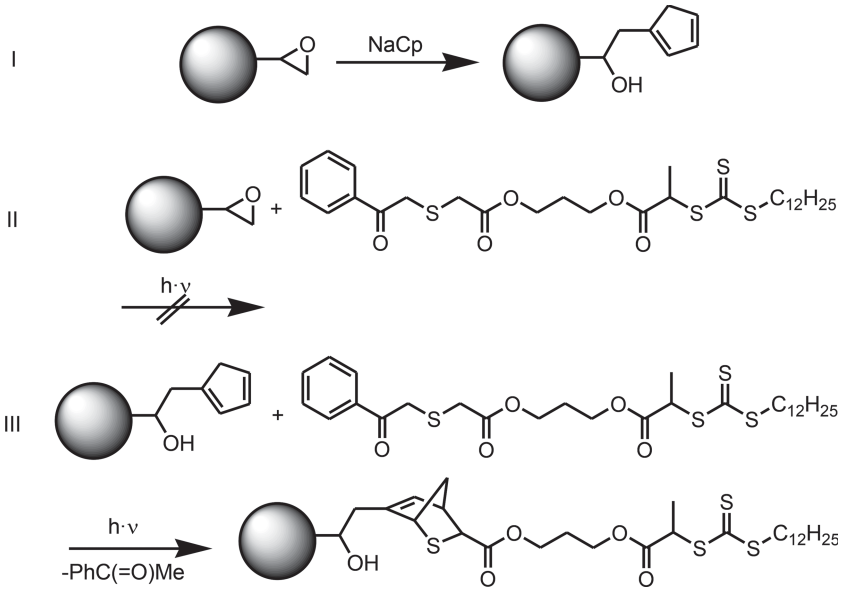

Figure 4. Top: Cyclopentadiene (Cp)-functionalization of PGMA microspheres employing sodium cyclopentadienide; middle: Control reaction between PGMA spheres and DoPATPAS; bottom: Test reaction between Cp-functional spheres and DoPATPAS.

altered by the reaction. In the current case, the microspheres have maintained their shape and structural integrity (refer to the Supporting Information, Figures S6–S8). In-depth chemical information can be gained via the elemental analysis (EA) and XPS. Although XPS is a surface analysis technique and EA gives information about the entire sample, both techniques essentially provide proof for the successful grafting experiment utilizing DoPATPAS. Only the XPS data on the test reaction revealed the presence of sulfur (1.6 at%) after successful grafting. The sulfur peak (**Figure 5**), can be deconvoluted into two doublets, one S $2p_{3/2}$ at 163.5 eV and one with S $2p_{3/2}$ at 164.9 eV (associated to the trithiocarbonate).[52] As expected, the control reaction shows only noise in the sulfur signal region, just as for the unaltered GMA spheres and Cp-functionalized spheres.

The elemental analysis of the reactions shows sulfur in both experiments (the full results of the elemental analysis can be found in the Supporting Information, Table S2). For the test reaction, a sulfur content of 0.53 wt% is observed, which is a clear and distinct increase. However, for the control reaction, the sulfur content is merely 0.13 wt%, which is only slightly higher than for the Cp-functionalized spheres (0.10 wt%). Such values for the sulfur content are within the error margin of the technique, and it is unknown if they are just artifacts or stemming from cross contamination, side reactions, or impurities. The sulfur content can be employed to calculate a loading capacity via Equation (1):

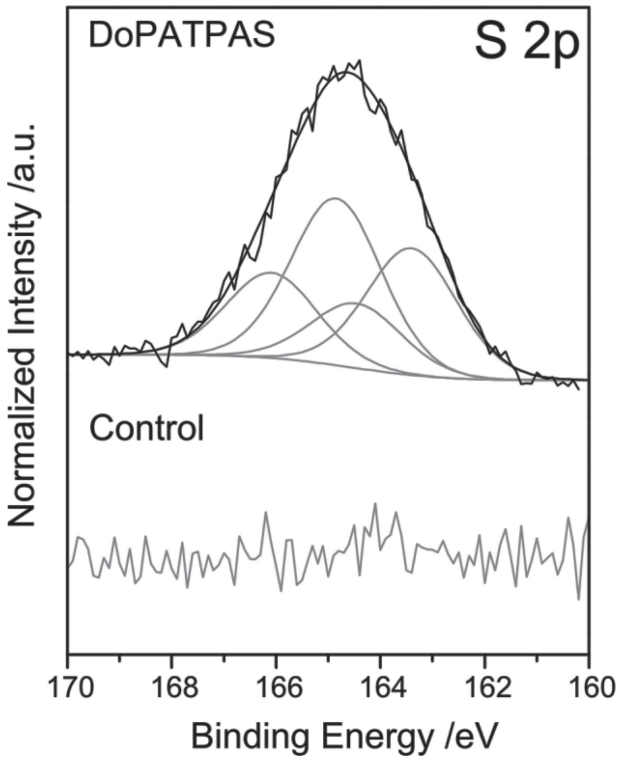

Figure 5. S 2p XP spectra of Cp-microspheres photografted with DoPATPAS (top) and of PGMA spheres subjected to the same reaction conditions (bottom). Only for the previously Cp-functionalized spheres sulfur can be detected.

$$LC = \frac{W(S)}{n(S)M(S)} \quad (1)$$

where LC is the loading capacity (in mol g^{-1}), W(S) is the weight of sulfur per 1 g of microspheres obtained via EA, n(S) is the number of sulfur atoms per grafted molecule (here 4) and M(S) is the molecular weight of sulfur. Employing Equation (1) leads to a loading capacity of 44.5 µmol g^{-1}. A loading capacity of 44.5 µmol g^{-1} is in excellent agreement with values obtained by grafting RAFT polymers via the also-phototriggered photo-enol approach, employing similar maleimide-functionalized porous microspheres (41.6 µmol g^{-1}).[25] Furthermore, the value is only slightly smaller than the loading capacities obtained by a thermally induced grafting reaction employing the RAFT-HDA approach (more than 150 µmol g^{-1} for reaction times of up to 5 days)[35] on microspheres that are also Cp-functionalized.

Via inverse size exclusion chromatography, the relative surface area of the (non-functionalized) PGMA starting material was determined to be close to 225.4 m^2 cm^{-3}. The density of the spheres has been reported to be close to 1.39 g cm^{-3}.[35,53] Thus, the surface area of the spheres is 1.62×10^{20} nm^2 g^{-1}. By employing the measured surface area the grafting density can be determined via Equation (2):

$$GD = \frac{W(S)N_A}{n(S)M(S)A} \quad (2)$$

where GD is the grafting density in chains per unit area; W(S) is the weight of sulfur in 1 g of microspheres obtained via elemental analysis, N_A is Avogadro's number, n(S) is the number of sulfur atoms per polymer chain, M(S) is the molecular weight of sulfur, and A is the measured surface area of the microspheres. Via the light-induced phenacyl sulfide-based reaction, a grafting density of close to 0.17 molecules per nm^2 is reached. The grafting density might even be higher as there is the possibility of a degradation of the trithiocarbonate group, although earlier results suggest that it is stable under the applied or similar conditions.[25,50,51]

In summary, it can be stated that the photogenerated thioaldehyde reacts in cycloaddition reactions with Cp-functionalized microspheres, which is verified via XPS and EA data. The grafting density and loading capacity calculated from the elemental constitution are in the same dimension as values obtained for similar (thermal and light-triggered) grafting reactions performed on functional porous microspheres.

2.3.2. Phototriggered Grafting of RAFT Polymers

In a similar fashion as for the test reaction, RAFT polymers (PS, PDMAA, and PAcManEA) can be grafted onto the microspheres. The Cp-functionalized microspheres and the RAFT polymer are mixed in DCM, the suspension is percolated with nitrogen and subsequently irradiated for 60 min (**Figure 6**). After intensive washing and drying (refer to the Experimental Section for details on the washing procedure), the particles are analyzed via SEM, XPS, EA and—in the case of grafted PDMAA—FT–IR microscopy.

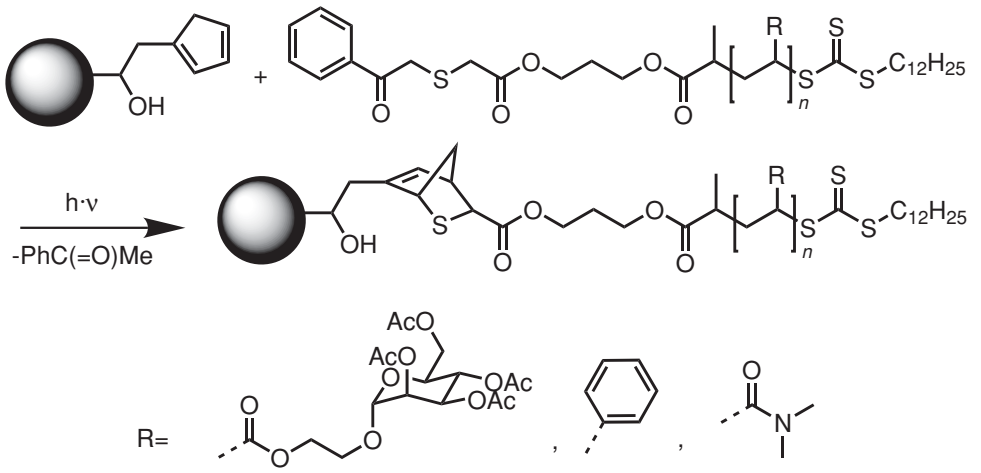

Figure 6. Phototriggered grafting reactions of RAFT polymers onto Cp-functionalized microspheres.

As noted above, the SEM analysis cannot prove a chemical transformation, yet it is important to demonstrate that no change in the shape and porosity of the spheres has occurred: For all grafted-on polymers no change can be observed (refer to the Supporting Information, Figure S9–S17).

Analysis of the XP spectra provides chemical information regarding the surface of the particles. No sulfur can be detected for the Cp-functionalized microspheres (**Figure 7**). For all grafted polymers there is a clear signal for sulfur (between 0.4 at% (PAcManEA) and 0.8 at% (PDMAA)), indicating a successful grafting reaction.

Sulfur can be found in the newly formed thiopyran ring as well as in the trithiocarbonate (S $2p_{3/2}$ at 163.4 eV and S $2p_{3/2}$ at 164.9 eV). In the cases of grafted-on PDMAA and PAcManEA, a third sulfur signal associated with oxidized sulfur (S $2p_{3/2}$ at 169.2 eV) can be identified. Such a signal has been found in the XP spectra of RAFT polymers before.[35,54]

For the unmodified PGMA microspheres only traces of nitrogen can be found in the XPS (0.4 at%; refer to **Figure 8**). The nitrogen most likely originates from the radical initiator or the stabilizer added during the particle synthesis. After the Cp-functionalization, the signal vanishes and only noise can be found in the area of the spectra associated with nitrogen. For microspheres grafted with PDMAA, a clear and distinct nitrogen signal can be detected stemming from the amide in the repeating unit (5.9 at%), further indicating the successful grafting of the polymer. Two species can be distinguished: one at 400.1 eV, which is attributed to the amide,[55] and one at 401.8 eV, which represents a protonated nitrogen.

The successful photografting of PS and PAcManEA can additionally be evidenced by a closer inspection of the C 1s signal in the XP spectra. The C 1s peak can be deconvoluted into several signals attributable to carbon atoms in different chemical environments (**Figure 9**). The signal at 285.0 eV is assigned to carbon bound to carbon or hydrogen (C–C, C–H) and the signal at 286.7 eV to carbon bound to oxygen (C–O). The third signal at 289.0 eV is associated with esters (O–C=O). For the grafted PDMAA, a fourth signal at 287.9 eV can be detected, which is associated with the amide functionality in the lateral polymer chain.[56] The peak attributed to (C–O, C–N) also shifts to a slightly smaller binding energy (286.4 eV) because of the amount of C–N bonds present in PDMAA.

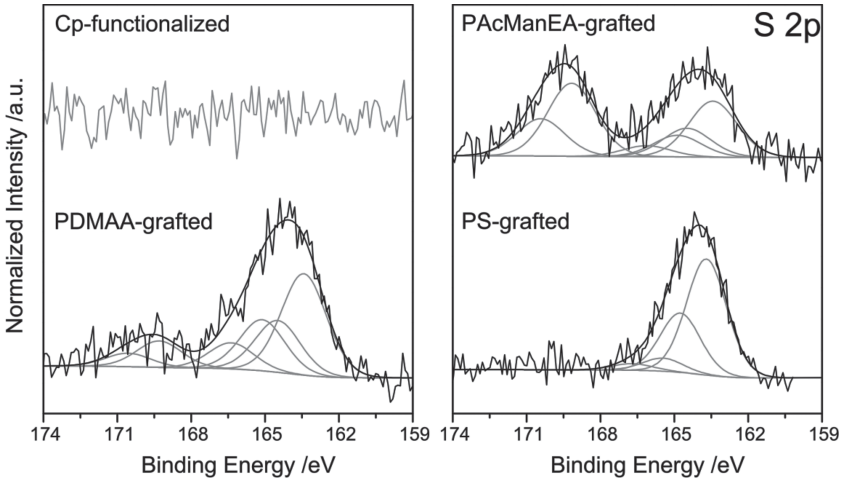

Figure 7. S 2p XP spectra of Cp-microspheres (top left) photografted with PAcManEA (top left), PDMAA (bottom left), and PS (bottom right). Sulfur can be detected in all samples after the photografting.

The ratio of the different carbon species in the C 1s peak are correlated to the chemical changes occurring in the reaction sequence and can thus now be employed to visualize the functionalization and grafting reactions. In particular, the ratio of the peaks belonging to carbon bound to oxygen or nitrogen (C–O, C–N) and carbon bound to carbon or hydrogen (C–C, C–H) effectively indicates the functionality change on the microspheres (**Figure 10**). The addition of small molecules, such as cyclopentadiene or the RAFT agent DoPATPAS, should not change the ratio of these signals significantly, yet the addition of cycloptentadiene (only consisting of carbon and hydrogen) leads to a slight

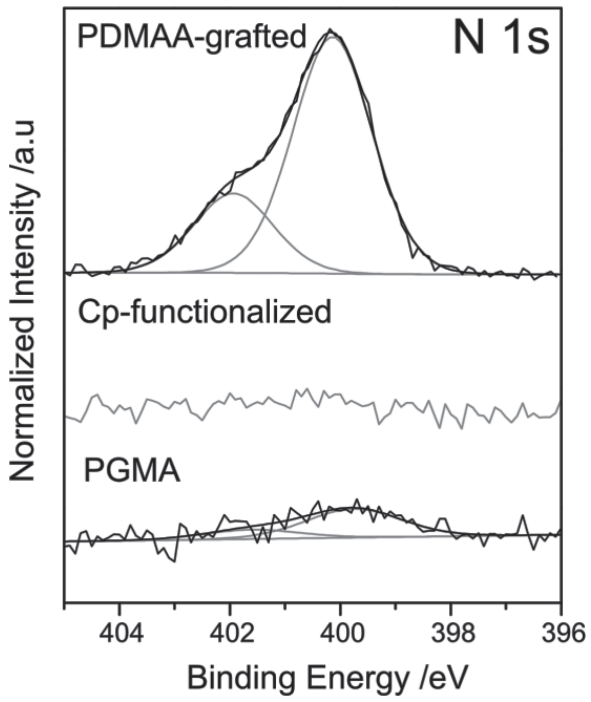

Figure 8. N 1s XP spectra of unmodified PGMA particles (bottom), Cp-functionalized microspheres (middle), and microspheres photografted with PDMAA (top). Only traces of nitrogen can be detected for unmodified particles; none can be found after Cp-functionalization and—as expected—a distinct nitrogen peak can be observed after the grafting. The increase of the nitrogen signal evidences the successful macromolecular grafting.

decrease of the ratio. The introduction of PDMAA, which has similar ratios of the concerned carbons in its repeating unit as PGMA, should also not significantly affect the ratio of the considered signals. In contrast, via the introduction of polystyrene (repeating unit only contains carbon and hydrogen) and PAcManEA (expressing many carbons bound to oxygen) onto the microsphere surface, the ratio should change significantly. Inspection of Figure 10 indicates that the change of the ratios exactly matches the theoretical expectation, again proving a successful light-induced grafting reaction employing the photoreactive RAFT polymers. For the error margins an estimated error of 10% was employed, which is associated with the accuracy of XPS analysis.

High resolution FT-IR microscopy can be employed to determine the spatial distribution as well as the amount of IR-active groups on microspheres[25,32] and on flat substrates.[57] Since PDMAA contains an amide exhibiting an IR band that can readily be distinguished from the ester vibration of the PGMA spheres, IR microscopy is an elegant tool to show the successful and evenly distributed grafting of PDMAA onto microspheres, as evidenced in **Figure 11**. By mapping the ester vibration close to 1750 cm^{-1} the microsphere can be imaged, showing its circular shape and the highest intensity in the middle of the sphere for the Cp-functionalized spheres as well as for the ones grafted with PDMAA. Imaging of the amide vibration at approximately 1650 cm^{-1} only returns noise for the Cp-functionalized sphere, whereas the same shape as well as intensity

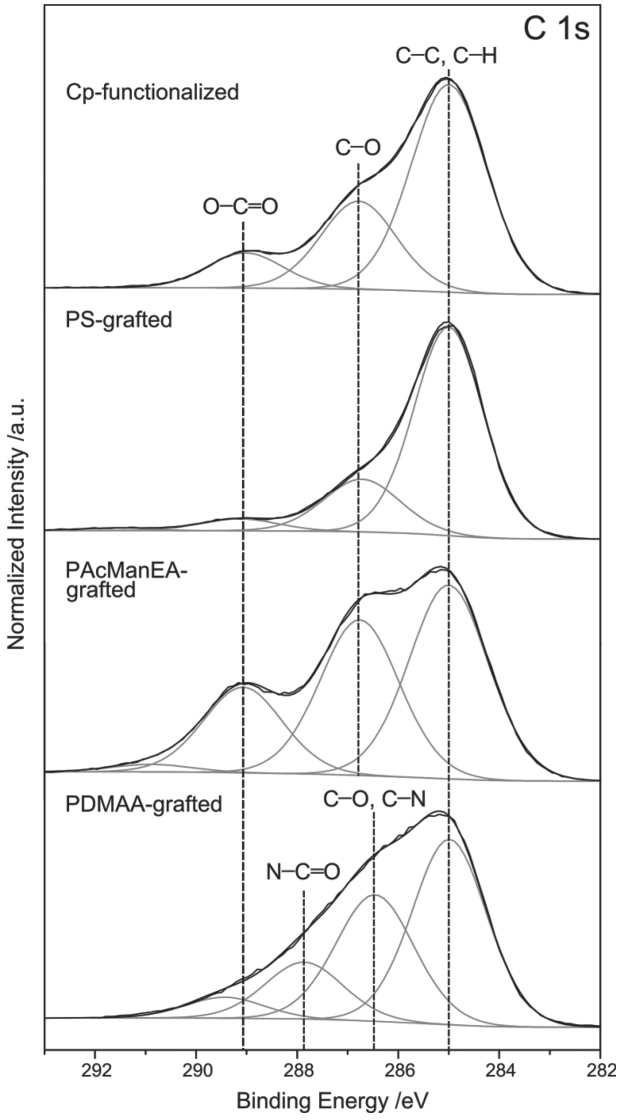

Figure 9. C 1s XP spectra of Cp-functionalized microspheres (top) and microspheres photografted with PS (2nd row), PAcManEA (3rd row), and PDMAA (bottom). The peaks are deconvoluted into signals stemming from chemically different carbon species.

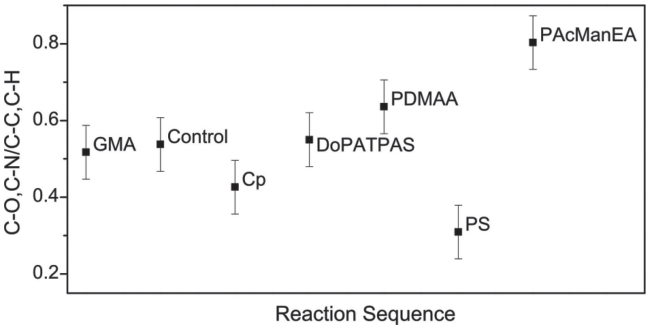

Figure 10. Comparison of the amount of carbon bound to oxygen or nitrogen and carbon bound to carbon or hydrogen based on the deconvolution of the carbon peak in the XP spectra (see also Figure 9 and Figure S18). The values are in agreement with the theoretically expected changes for grafted-on polymers.

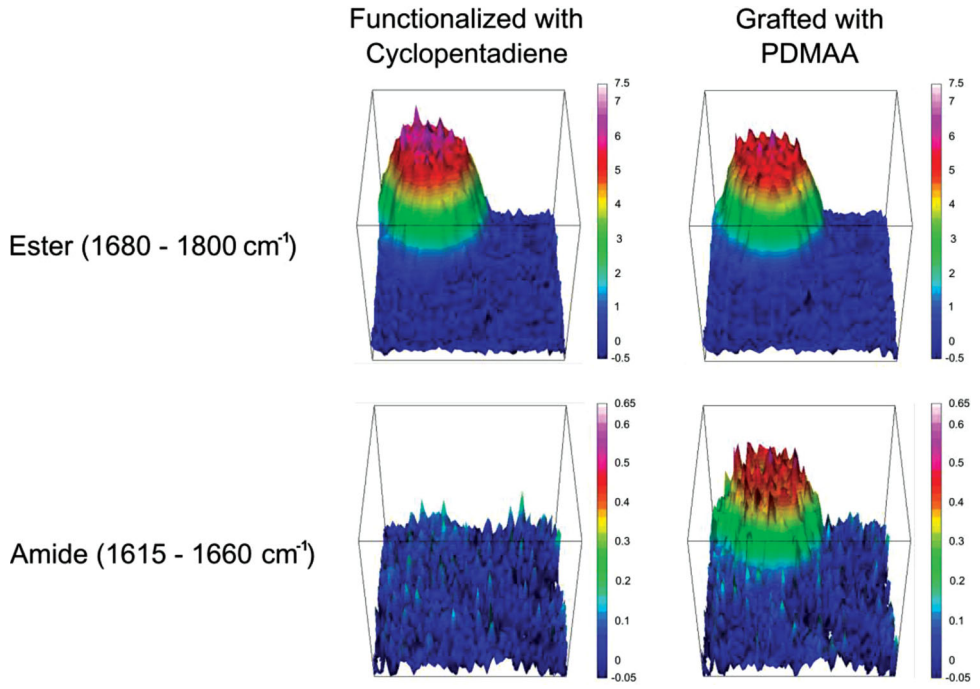

Figure 11. False-color, high-resolution FT-IR-microscopy images (4 cm^{-1} spectral resolution with a pixel resolution of 0.25 μm^2) of a cycloptentadiene-functionalized PGMA microsphere before and after photografting of PDMAA. The measured area is 32 μm × 32 μm. Red corresponds to a high degree of functionalization. In the top row, the intensity of bands corresponding to the O–C=O stretching vibration is visualized, in the bottom row the N–C=O bands.

distribution can be found for the particle with PDMAA, again confirming successful grafting.

Quantitative information regarding the grafting onto microspheres can be obtained via elemental analysis. To quantify the grafting efficiency the sulfur content is employed, as sulfur is an element which is only introduced into the particles via a successful grafting reaction. Furthermore, sulfur is only present in the chain end-groups, thereby eliminating any errors of the loading capacity or grafting density associated with inaccuracies in the chain length of the grafted polymers. For grafted PS, a sulfur content of 0.24 wt% is observed, for PDMAA 0.33 wt%, and for PAcManEA 0.16 wt%. Applying Equation (1) and Equation (2) leads to loading capacities and grafting densities of 18.7 μmol g^{-1} and 0.07 molecules nm^{-2} for grafted PS, 25.7 μmol g^{-1} and 0.10 molecules nm^{-2} for grafted PDMAA, and 10.1 μmol g^{-1} and 0.05 molecules nm^{-2} for PAcManEA. Inspection of these numbers indicates a significant decrease of the grafting density with the chain length of the grafted glycopolymer, suggesting that steric hindrance is limiting the achievable grafting density. The grafting densities obtained using the current phenacyl sulfide photografting approach are in excellent agreement with the values obtained by a different phototriggered grafting reaction, the photo-enol approach, leading to grafting densities of around 0.1 molecules nm^{-2} with polymers similar in structure and chain length.[25]

By combining the data from the elemental analysis and XPS measurements, a complete picture of the photo-induced grafting can be constructed. Although XPS is mainly a surface analysis tool with penetration depths in the range of five to ten nanometers while elemental analysis gives information about the entire sample, they both lead to the same conclusions. Figure S18 in the Supporting Information shows a comparison of the nitrogen contents derived from EA and XPS (for the error margins in the EA, the standard deviation of the measurements was employed, for XPS an error of 10% was estimated).

XPS shows only noise for all samples, with the exception of the spheres photografted with PDMAA. Via elemental analysis, some nitrogen traces can be found in every sample, as it can stem from the radical initiator, stabilizer, porogen, impurities, or even trapped atmospheric nitrogen. Nevertheless, a distinct and unambiguous increase in the nitrogen content can be seen for grafted PDMAA. An identical result is obtained for the sulfur content when comparing XPS and EA, as illustrated in **Figure 12**.

The highest sulfur content is found in the test reaction, where the novel photoreactive RAFT agent DoPATPAS was grafted onto Cp-functionalized microspheres. The untreated spheres show no sulfur content in both techniques. The Cp-functionalized spheres as well as the test reaction employing unfunctionalized PGMA spheres show no sulfur content via XPS and only low quantities in the elemental analysis. For all the grafted-on polymers, sulfur can be detected with the highest amount found for PDMAA and the lowest for PAcManEA, which had the highest molecular weight and therefore also the largest steric hindrance, impeding the grafting of the chains.

In summary, the photo-induced grafting of RAFT polymers onto Cp-functionalized porous microspheres employing thioaldehyde ligation was successful utilizing a single-photon irradiation process, as evidenced via XPS, FT-IR microscopy, and elemental analysis. Determined grafting densities are comparable

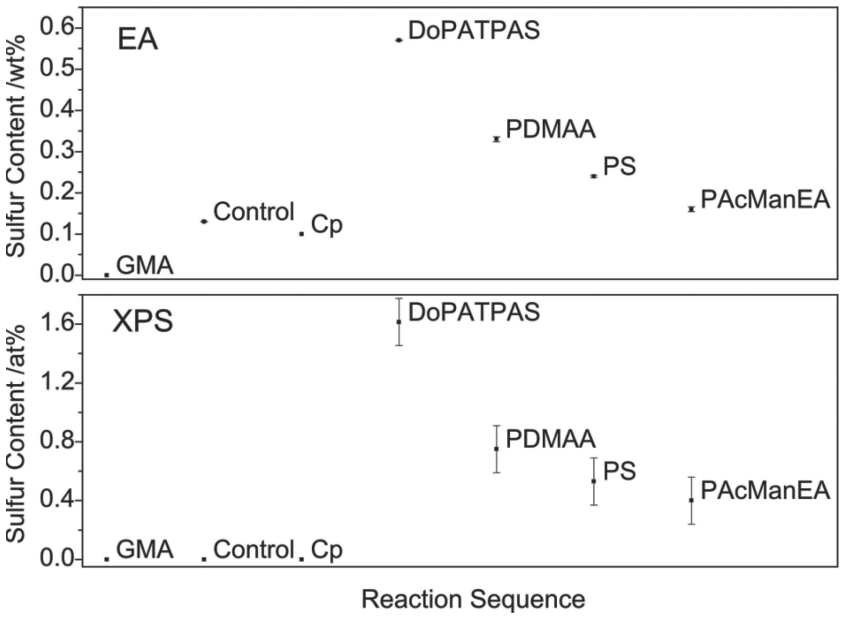

Figure 12. Comparison of the sulfur contents derived from elemental (top) and XPS (bottom) analysis of all microsphere samples.

to previously reported values obtained via light-induced immobilization techniques on polymeric particles.[25]

2.4. Spatially Resolved Grafting via Direct Laser Writing

To illustrate the universality of thioaldehyde ligation, the photofunctional RAFT polymers were also tethered to nucelophilic planar surfaces in a spatially resolved fashion, applying a two-photon direct laser writing (DLW) process.

2.4.1. Coating with PDA

PDA was deposited from a 2 mg mL^{-1} solution prepared by the dissolution of dopamine hydrochloride in an air-saturated 10 mM Tris-HCl (pH 8.5) buffer.[36] Glass slides and silicon wafers were coated via the autopolymerization of dopamine in aqueous solution in the presence of the respective substrate. The thickness of the PDA layer is 16.8 ± 2.1 nm, determined via spectroscopic ellipsometry. Since dopamine contains an amine group, the surface exhibits a significant amount of nucleophilic groups[58–60] that can be employed for further grafting reactions, in particular, with phenacyl sulfides (**Figure 13**).

2.4.2. Spatially Resolved Surface Patterning of RAFT Polymers onto PDA Interfaces

For direct surface patterning, a droplet of polystyrene containing thioaldehyde precursor in ε-caprolactone was placed onto a PDA-functionalized glass slide or silicon wafer. The functionalized side of the substrate was then covered with another glass slide. Thus, the droplet was located between the cover glass slide and the substrate. Subsequently, the sample was inserted into the direct laser writing (DLW) setup and surface patterning was performed by focusing the laser beam through the glass slide and the reaction mixture directly onto the PDA-functionalized surface. With this technique, surface patterning of non-transparent substrates (such as silicon wafers) is possible. Light-induced surface modification was performed utilizing different patterns, such as squares (40 × 40 µm with an interval of 10 µm) or the logo of the KIT (20 × 55 µm), were written with the DLW setup, as described in the Experimental Section.

The surfaces grafted with the RAFT polymer were analyzed by time-of-flight secondary ion mass spectrometry (ToF-SIMS), allowing for the imaging of the surface functionalization on the micrometer scale. The successful local grafting of the polystyrene chains was proven by imaging the lateral distribution of the tropyl cation, together with other characteristic PS-derived ions (**Figure 14**).

The DLW technology provides small patterns with high fidelity yielding sharp structures as depicted in Figure 14 left and center. The $C_7H_7^+$ intensity profile across a patterned line obtained from the analysis shown in Figure 14 right demonstrates a lateral resolution better than 1 µm based on the (80/20) definition (Figure S20). Notably, virtually any 2D structure can be written onto a PDA-coated surface employing the

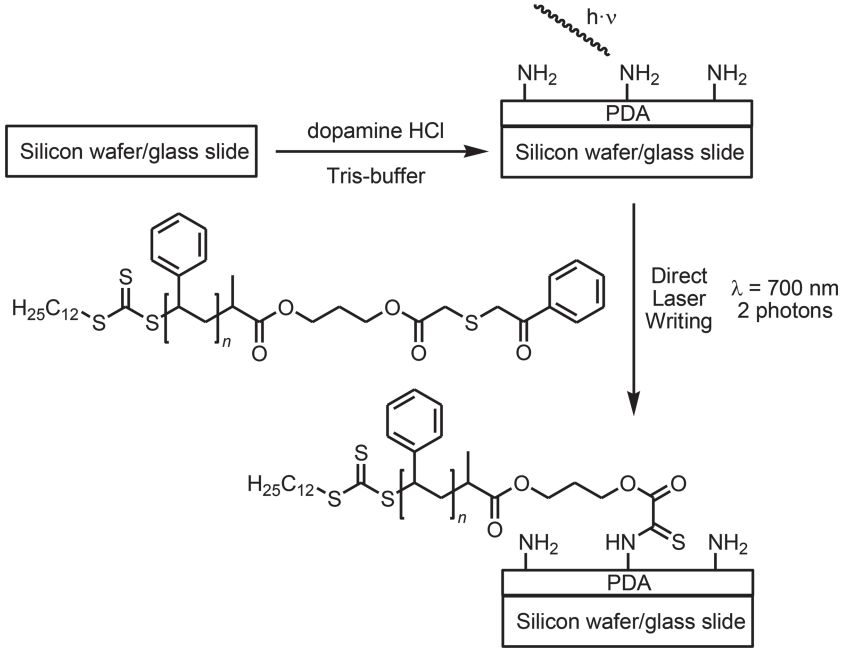

Figure 13. Synthetic route for the photopatterning of PDA interfaces.

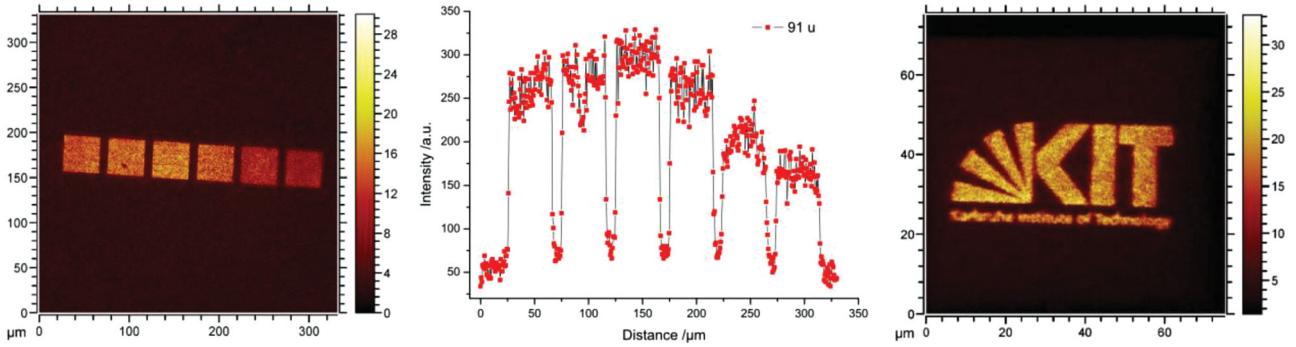

Figure 14. ToF-SIMS imaging of the $C_7H_7^+$ ion from PS grafted onto a PDA-functionalized silicon wafer (left). Imaging of the sum of $C_7H_7^+$, $C_8H_9^+$, $C_9H_7^+$ and $C_9H_9^+$ signals from PS grafted onto a PDA-functionalized glass slide by DLW (right). The diagram in the center depicts the 'intensity profile' for the $C_7H_7^+$ signal across the squares of the DLW patterned structure, shown left visualizing the lateral resolution of the obtained structures.

procedure described here. As an example, the logo of KIT was chosen (Figure 14 right). The high spatial resolution that was achieved is an indication of a very fast grafting process. The possibility to functionalize PDA surfaces in a spatially resolved fashion is particularly interesting, as PDA can be applied to a vast range of surfaces, enabling precise grafting of a range of polymers via DLW. Furthermore, the phenacyl sulfide reaction is not restricted to macromolecules, providing the possibility to graft small molecules such as orthogonal functional groups or even ligands to the PDA surface.

3. Conclusions

The synthesis and application of a novel RAFT agent carrying a phenacylsulfide, which forms a thioaldehyde when irradiated with light (λ_{max} = 355 nm) is introduced. RAFT polymerization of styrene and dimethylacrylamide was conducted, reaching dispersities below 1.1 for M_n of 3600 and 4800 g mol^{-1}. In addition, a protected glycopolymer was synthesized with $Đ$ = 1.2 (M_n = 15 000 g mol^{-1}). All polymers show high end-group fidelity. The photogenerated thioaldehyde on the chain ends can undergo hetero Diels–Alder reactions with dienes as well as reactions with nucleophiles. Subsequently, the RAFT polymers were photoligated to porous polymeric microspheres, previously functionalized with cycloptentadiene moieties. The grafted particles were thoroughly characterized via SEM, elemental analysis, XPS, and high-resolution FT-IR-microscopy, leading to qualitative as well as quantitative information about the reaction efficiency. Grafting densities up to 0.10 molecules nm^{-2} were reached. The versatility of the thioaldehyde ligation is further evidenced by the spatially resolved grafting of polystyrene onto poly(dopamine)-coated glass slides and silicon wafers via two-photon direct laser writing. The polydopamine layers, which exhibit a significant amount of nucleophilic amine groups, can be applied on any surface. The DLW approach allows for the generation of virtually any (two-dimensional) polymer pattern to be grafted. In summary, the combination of thioaldehyde ligation, RAFT polymerization, PDA coated surfaces, and DLW allows the spatially resolved grafting of a vast range of polymers onto various substrates in any desired pattern.

4. Experimental Section

4.1. Materials

1-((3-Hydroxypropoxy)carbonyl)ethyl dodecyl carbonotrithioate (DoPATOH), (phenacyl-thio)acetic acid,[16] and 2-(2',3',4',6'-Tetra-*O*-acetyl-*β*-D-mannosyloxy) ethylacrylate (AcManEA)[25] were synthesized according to the literature. 2,2'-Azobis(2-methylpropionitrile) (AIBN) was recrystallized twice from methanol. Styrene and *N*,*N*-dimethylacrylamide (DMAA) were passed through a column of basic alumina to remove inhibitor and subsequently stored at -19 °C. Dichloromethane (DCM) was dried and stored over $CaCl_2$. Poly(glycidyl methacrylate) (PGMA) microspheres with a PGMA content of 80% and pore size of 1000 Å were synthesized by Polymer Standards Service (PSS) GmbH and functionalized with cycloptentadiene moieties as described in a previous publication.[35] All other chemicals were used as supplied by the manufacturers.

4.2. Synthesis of DoPAT-Phenacylsulfide (DoPATPAS)

DoPATOH (1.537 g, 3.76 mmol, 1.00 equiv), (phenacylthio)acetic acid (872 mg, 4.15 mmol, 1.10 equiv) and 4-dimethylaminopyridine (9.1 mg, 0.075 mmol, 0.02 equiv) were dissolved in 10 mL dry DCM (dried over $CaCl_2$). The solution was cooled to 0 °C in an ice bath and dicyclohexylcarbodiimide (990 mg, 4.80 mmol, 1.28 equiv) dissolved in 4 mL dry DCM was added dropwise. The reaction was covered with aluminum foil to protect it from ambient light. After 1 h, the ice bath was removed and the reaction proceeded over night at ambient temperature. After filtration, the organic layer was washed with 5% HCl, saturated $NaHCO_3$ solution and distilled water, dried over Na_2SO_4 and the solvent removed. The crude product was purified via column chromatography (silica gel, cyclohexane/ethyl acetate 4:1) to afford a yellow oil (1.792 g, 79 %). ^{1}H NMR (400 MHz, $CDCl_3$, δ): 7.96 (d, ^3J = 7.3 Hz, 2H, orthoAr), 7.59 (t, ^3J = 7.3 Hz, 1H, paraAr), 7.48 (t, ^3J = 7.5 Hz, 2H, metaAr), 4.80 (q, ^3J = 7.4 Hz, 1H, $SC\underline{H}CH_3$), 4.21 (m, 4H, $C(O)OC\underline{H}_2CH_2C\underline{H}_2OC(O)$), 4.02 (s, 2H, $ArC(O)C\underline{H}_2SCH_2$), 3.33 (m, 4H, $ArC(O)CH_2S\underline{CH}_2$ and $SC\underline{H}_2CH_2C_7H_{14}CH_2CH_2CH_3$), 1.99 (quin, ^3J = 6.0 Hz, 2H, $C(O)OCH_2C\underline{H}_2CH_2OC(O)$), 1.68 (quin, ^3J = 7.4 Hz, 2H, $SCH_2C\underline{H}_2C_7H_{14}CH_2CH_2CH_3$), 1.59 (d, ^3J = 7.4 Hz, 3H, $SCHC\underline{H}_3$), 1.38 (m, 2H, $SCH_2CH_2C_7H_{14}CH_2C\underline{H}_2CH_3$), 1.25 ($s_{br}$, 16H, $SCH_2CH_2C_7\underline{H}_{14}C\underline{H}_2CH_2CH_3$), 0.87 (t, ^3J = 6.8 Hz, 3H, $SCH_2CH_2C_7H_{14}CH_2CH_2C\underline{H}_3$); ^{13}C NMR (100 MHz, $CDCl_3$, δ): 222.0 (SC(S)S), 193.9 ($ArC(O)CH_2SCH_2$), 171.0 ($SCH(CH_3)\underline{C}(O)O$), 169.7 ($SCH_2\underline{C}(O)O$), 135.3 (substituted Ar), 133.5 (paraAr), 128.7 (orthoAr), 128.6 (metaAr), 62.1 ($SCH(CH_3)C(O)O\underline{C}H_2$), 61.8 ($SCH_2C(O)O\underline{C}H_2$), 47.8 ($S\underline{C}HCH_3$), 37.7 ($S\underline{C}H_2C(O)O$), 37.3 ($S\underline{C}H_2CH_2C_7H_{14}CH_2CH_2CH_3$), 33.3 ($ArC(O)O\underline{C}H_2$), 31.9 ($SCH_2CH_2C_7H_{14}\underline{C}H_2CH_2CH_3$), 29.6, 29.5 (2x), 29.4, 29.3, 29.0, 28.9, 27.8, (8C, $SCH_2\underline{C}H_2\underline{C}_7H_{14}CH_2CH_2CH_3$),

27.7 ($C(O)OCH_2\underline{C}H_2CH_2C(O)O$), 22.7 ($SCH_2CH_2C_7H_{14}CH_2\underline{C}H_2CH_3$), 16.7 ($SCH\underline{C}H_3C(O)O$), 14.1 ($SCH_2CH_2C_7H_{14}CH_2CH_2\underline{C}H_3$); UV–vis (acetonitrile): λ_{max} = 307, 240 nm; MS (ESI) *m/z*: $[M+Na]^+$ calcd for $C_{29}H_{44}O_5S_4$: 623.19, found 623.24.

4.3. RAFT Polymerizations

Synthesis of Polystyrene (PS): A solution of AIBN (4.2 mg, 0.026 mmol, 0.10 equiv) and DoPATPAS (156.1 mg, 0.26 mmol, 1.00 equiv) in styrene (2.98 g, 28.5 mmol, 110 equiv) was deoxygenated with four consecutive freeze-pump-thaw cycles. The reaction was placed into a preheated oil-bath at 60 °C for 14.5 h. The reaction was stopped by cooling in an ice-bath and exposing the reaction mixture to oxygen. The remaining styrene was removed via evaporation at ambient conditions and the polymer isolated via precipitation in cold methanol and subsequent drying under vacuum to afford 774 mg of a slightly yellow powder. Conversion = 33% (gravimetry); M_n = 3600 g mol^{-1}, $Đ$ = 1.08 (GPC in THF, polystyrene calibration); M_n = 3650 g mol^{-1} (NMR, comparison of the integrals between 8.05–7.90 ppm and 7.36–6.25 ppm).

Synthesis of Poly(N,N-dimethylacrylamide) (PDMAA): A solution of AIBN (9.4 mg, 0.057 mmol, 0.20 equiv), DoPATPAS (174.1 mg, 0.29 mmol, 1.00 equiv) and DMAA (1.47 g, 14.8 mmol, 51 equiv) in DMF (7.5 mL) was deoxygenated with four consecutive freeze-pump-thaw cycles. The reaction was placed into a preheated oil-bath at 60 °C for 3 h. The reaction was stopped by cooling in an ice-bath and exposing the reaction mixture to oxygen. The polymer was isolated by dialyzing the reaction mixture against distilled water (utilizing a SpectraPor3 membrane (MWCO = 500 Da)) and subsequent freeze drying to give 1.10 g of a yellow solid. M_n = 7200 g·mol^{-1}, $Đ$ = 1.07 (GPC in dimethylacetamide (DMAc), polystyrene calibration); M_n = 4800 g·mol^{-1} (NMR, comparison of the integrals between 8.05–7.90 ppm and 3.15–2.60 ppm).

Synthesis of Poly(2-(2′,3′,4′,6′-tetra-O-acetyl-β-d-mannosyloxy) ethylacrylate) (PAcManEA): A solution of AIBN (5 mg, 0.03 mmol, 0.19 equiv), DoPATPAS (94.1 mg, 0.157 mmol, 1.00 equiv) and AcManEA (3.47 g, 7.77 mmol, 50 equiv) in DMAc (15 mL) was deoxygenated with four consecutive freeze-pump-thaw cycles. The reaction was placed into a preheated oil-bath at 60 °C for 8 h. The reaction was stopped by cooling in an ice-bath and exposing the reaction mixture to oxygen. The polymer was isolated by precipitation in cold diethyl ether and dried under vacuum to give 1642 mg of a slightly yellow, waxy solid (precipitation was not quantitative). M_n = 6200 g mol^{-1}, $Đ$ = 1.20 (GPC in DMAc, polystyrene calibration); M_n = 15 000 g mol^{-1} (NMR, comparison of the resonance integrals between 8.05–7.90 ppm and 5.40–3.60 ppm).

4.4. Functionalization of Silicon Wafers and Glass Slides with Polydopamine (PDA)

Substrate Preparation: One side polished silicon wafers with a 50 nm thermal silicon dioxide (SiO_2) over-layer and BK-7 glass slides were sonicated in methanol and deionized water (Milli Q system, Millipore) for 15 min, immersed in a mixture of 25% ammonia, 30% hydrogen peroxide and water (1:1:5 v/v/v) heated at 70 °C for 10 min and finally thoroughly rinsed with water. Dry samples were exposed to air plasma (25 W) for 5 min just before PDA deposition.

Polydopamine (PDA) Coating: PDA was deposited from a 2 mg mL^{-1} solution prepared by dissolution of dopamine hydrochloride in an air-saturated 10 mM tris(hydroxymethyl)aminomethane-HCl (pH 8.5) buffer.[36] The deposition of PDA on the Si-substrates was performed in open glass dishes and under controlled stirring that provided a continuous supply of oxygen through the air/solution interface. In addition, the flat substrates were kept vertical to suppress microparticle sedimentation.[38,41,58] The coated surfaces were finally rinsed with water, sonicated in water for 15 min and dried in a stream of nitrogen.

Table 1. Details and Weigh-ins of Control and Grafting Reactions on Microspheres (MS).

Type of MS (amount)	Grafted molecule (amount)
GMA (100.6 mg)	DoPATPAS (60.7 mg)
Cp (100.4 mg)	DoPATPAS (61.0 mg)
Cp (100.1 mg)	PS (360.5 mg)
Cp (100.8 mg)	PAcManEA (629.3 mg)
Cp (99.9 mg)	PDMAA (470.2 mg)

4.5. Photoreactions

Grafting Reactions and Control Reaction on Microspheres: The microspheres and DoPATPAS or RAFT polymer, respectively, were mixed in DCM (5 mL) in glass vials (Pyrex, diameter 20 mm), which were crimped airtight with styrene/butadiene rubber seals (refer to **Table 1** for details). The mixture was deoxygenated via purging with nitrogen for 20 min. The vials were subsequently irradiated for 60 minutes by rotating around a compact low-pressure fluorescent lamp (Philips CLEO Compact PL-L, λ_{max} = 355 nm) at a distance of 40–50 mm in a custom built photoreactor (refer to the Supporting Information, Figure S5 for details). The microspheres were filtered off and washed three times with DCM and dried for four days at 50 °C under vacuum prior to analysis.

Direct Laser Writing: Direct laser writing experiments were conducted using a home-built setup that has been previously described in detail.[61] The setup is based on a Chameleon Ultra II, Coherent. The pulses were focused to a diffraction-limited spot by a 100× oil-immersion microscope lens (Leica HCX PL APO 100/1.4–0.7 CS Oil) with numerical aperture NA = 1.4. To write patterns, the samples were scanned with respect to the fixed focus by means of piezoelectric actuators. The pulse-picker described in the reference has been removed resulting in a repetition rate of 80 MHz and the laser has been tuned to 700 nm center wavelength. Patterning experiments were conducted using laser powers ranging from 8 mW to 3 mW and a writing speed of 100 µm s^{-1}. For the patterns depicted in Figure 14: the squares (left) were functionalized (left to right) employing laser powers ranging from 8 mW to 3 mW in 1 mW steps. For the KIT logo (right) a laser power of 6 mW was employed.

4.6. Analysis

Gel Permeation Chromatography (GPC): GPC measurements were performed on a Polymer Laboratories PL-GPC 50 Plus Integrated System, comprising an autosampler, a PLgel 5 mm bead-size guard column (50 × 7.5 mm) followed by three PLgel 5 mm MixedC columns (300 × 7.5 mm) and a differential refractive index detector using THF at 35 °C or *N,N*-dimethylacetamide (DMAc) containing 0.3% LiBr at 50 °C as the eluent with a flow rate of 1 mL min^{-1}. The GPC system was calibrated using linear polystyrene standards ranging from 476 to 2.5 × 10^6 g mol^{-1}. All GPC calculations were carried out relative to polystyrene calibration (Mark-Houwink parameters K = 14.1 × 10^{-5} dL g^{-1}, α = 0.70).[62]

Scanning Electron Microscopy (SEM): The morphology of the microspheres was studied on a Zeiss Supra 55. The samples were sputter-coated with 30 nm of gold before the measurement.

Electrospray Ionization-Mass Spectrometry (ESI-MS): Spectra were recorded on an LXQ mass spectrometer (Thermo-Fisher Scientific, San Jose, CA) equipped with an atmospheric pressure ionization source operating in the nebulizer assisted electrospray mode. The instrument was calibrated in the *m/z* range 195–1822 using a standard containing caffeine, Met-Arg-Phe-Ala acetate (MRFA) and a mixture of fluorinated phosphazenes (Ultramark 1621) (all from Aldrich). A constant spray voltage of 6 kV was used and nitrogen at a dimensionless sweep gas flow rate of 2 (approximately 3 L min^{-1}) and a dimensionless sheath gas flow rate of 5 (approximately 0.5 L min^{-1}) were applied. The capillary voltage, the tube lens offset voltage and the capillary temperature were set to 10 V, 70 V and 300 °C respectively. The samples were dissolved

with a concentration of 0.1 mg mL^{-1} in a mixture of THF and MeOH (3:2) containing 100 µmol of sodium triflate and infused with a flow of 10 µL min^{-1}.

Nuclear Magnetic Resonance (NMR) Spectroscopy: NMR measurements were conducted on a Bruker Ascend 400 at 400 MHz for hydrogen nuclei. Samples were dissolved in $CDCl_3$ or DMSO-d_6 using residual solvent peaks for shift correction.

X-Ray Photoelectron Spectroscopy (XPS): XPS investigations were performed on a K-Alpha spectrometer (Thermo Fisher Scientific, East Grinstead, UK) using a micro-focused, monochromated Al Kα X-ray source (400 µm spot size). The kinetic energy of the electrons was measured by a 180° hemispherical energy analyzer operated in the constant analyzer energy mode (CAE) at 50 eV pass energy for elemental spectra. The photoelectrons were detected at an emission angle of 0° with respect to the normal of the sample surface. The K-Alpha charge compensation system was employed during analysis, using electrons of 8 eV energy and low-energy argon ions to prevent any localized charge build-up. Data acquisition and processing using the Thermo Avantage software is described elsewhere.[63] The spectra were fitted with one or more Voigt profiles (BE uncertainty: (±0.2 eV)). The analyzer transmission function, Scofield[64] sensitivity factors, and effective attenuation lengths (EALs) for photo-electrons were applied for quantification. EALs were calculated using the standard TPP-2 M formalism.[65] All spectra were referenced to the C 1s peak of hydrocarbon at 285.0 eV binding energy, controlled by means of the well-known photo-electron peaks of metallic Cu, Ag, and Au.

Elemental Analysis (EA): The elemental composition of the microsphere samples was analyzed using an automatic elemental analyzer Flash EA1112 from Thermo Scientific, which was equipped with a MAS 200R auto sampler. More details can be found in the supporting information in ref. [53]

High-Resolution Attenuated Total Reflectance (ATR) FT-IR Microscopy Imaging: Infrared measurements were performed using a Bruker FT-IR microscope HYPERION 3000 coupled to a research spectrometer VERTEX 80. The HYPERION 3000 microscope is equipped with two types of detectors: a single element MCT-detector (Mercury Cadmium Telluride) for the conventional mapping approach and a multi-element FPA detector (focal plane array) for imaging. The FPA detector was used for the laterally resolved measurements. The multielement FPA detector consists of 64 × 64 elements. This allows for the simultaneous acquisition of 4096 spectra covering a sample area of 32 × 32 mm (for ATR detection). With the FPA-detector in combination with the 20× Germanium ATR-lens, a lateral pixel resolution of 0.25 μm^2 is achieved, with the optical resolution depending on the employed wavelength (1000 cm^{-1} to ~1 µm lateral resolution). For postprocessing baseline correction and atmospheric compensation were employed.

Time-of-Flight Secondary Ion Mass Spectrometry (ToF-SIMS): ToF-SIMS was performed on a TOF.SIMS5 instrument (ION-TOF, Münster, Germany) equipped with a Bi cluster liquid metal primary ion source and a nonlinear time-of-flight analyzer. For chemical surface characterization the Bi source was operated in the "bunched" mode, providing 0.7 ns Bi_3^+ ion pulses at 25 keV energy and a lateral resolution of ~4 µm. Negative polarity spectra were calibrated on the C^-, CH^-, and CH_2^- peaks. Positive polarity spectra were calibrated on the C^+, CH^+, CH_2^+, and CH_3^+ peaks. Primary ion doses for spectrometry were kept below 10^{11} ions cm^{-2} (static SIMS limit). After having established the chemical assignments from spectrometry data, high lateral resolution images were obtained applying the "burst alignment mode" of the primary ion source. This mode of operation avoids chromatic aberration of the Bi primary ion beam therefore provides a highly focused ion beam allowing for sub-µm lateral resolutions. Charge compensation was obtained by applying an electron flood gun providing electrons of 21 eV and tuning the secondary ion reflectron accordingly.

Ultraviolet–Visible (UV–vis) Spectroscopy: UV-Vis spectra were recorded on a Varian Cary 300 Bio spectrophotometer. Spectra were recorded in acetonitrile in a 10 mm path length cell. Spectra were collected between 200 and 800 nm. Samples were baseline corrected with respect to the pure solvent.

Spectroscopic Ellipsometry: The thickness of the films in the dry state was determined by ellipsometry using a Variable Angle Spectroscopic Imaging Auto-Nulling Ellipsometer EP3-SE (Nanofilm Technologies GmbH, Germany) in the wavelength range of λ = 399–811 nm (source Xe-arc lamp, wavelength step ~ 10 nm) at an angle of incidence AOI = 70° in air at room temperature. The optical constants of the PDA layers and SiO_2/Si substrates were taken from elsewhere.[38,66]

Supporting Information

Supporting Information is available from the Wiley Online Library or from the author.

Acknowledgements

C.B.-K. acknowledges continued funding from the Karlsruhe Institute of Technology (KIT) supporting the current project including support from the Helmholtz association via the STN program. C.R-E thanks the Alexander von Humboldt Foundation for financial support via Humboldt Research Fellowships for Postdoctoral researchers. C.R-E and O.P-G thank the Grant Agency of the Czech Republic (GACR), Contract No. P205–12–1702 and P108/11/1857. The authors thank Dr. Thorsten Hofe and the Polymer Standards Service GmbH for the provision of the PGMA microspheres, the Fraunhofer-Institut für Chemische Technologie ICT in Pfinztal for measuring the elemental analysis as well as Udo Geckle from the Institute for Applied Materials – Energy Storage System (IAM-ESS) at the KIT for the SEM measurements.

Received: February 21, 2014
Revised: May 9, 2014
Published online: July 14, 2014

[1] C. Rodriguez-Emmenegger, C. M. Preuss, B. Yameen, O. Pop-Georgievski, M. Bachmann, J. O. Mueller, M. Bruns, A. S. Goldmann, M. Bastmeyer, C. Barner-Kowollik, *Adv. Mater.* **2013**, *25*, 6123.
[2] F. Huo, Z. Zheng, G. Zheng, L. R. Giam, H. Zhang, C. A. Mirkin, *Science* **2008**, *321*, 1658.
[3] D. Mark, S. Haeberle, G. Roth, F. von Stetten, R. Zengerle, *Chem. Soc. Rev.* **2010**, *39*, 1153.
[4] C. M. Nimmo, M. S. Shoichet, *Bioconjugate Chem.* **2011**, *22*, 2199.
[5] A. W. Martinez, S. T. Phillips, G. M. Whitesides, E. Carrilho, *Anal. Chem.* **2009**, *82*, 3.
[6] J. S. Clovis, A. Eckell, R. Huisgen, R. Sustmann, *Chem. Ber.* **1967**, *100*, 60.
[7] E. Blasco, M. Piñol, L. Oriol, B. V. K. J. Schmidt, A. Welle, V. Trouillet, M. Bruns, C. Barner-Kowollik, *Adv. Funct. Mater.* **2013**, *23*, 4011.
[8] M. Dietrich, G. Delaittre, J. P. Blinco, A. J. Inglis, M. Bruns, C. Barner-Kowollik, *Adv. Funct. Mater.* **2012**, *22*, 304.
[9] R. K. V. Lim, Q. Lin, *Acc. Chem. Res.* **2011**, *44*, 828.
[10] T. Gruendling, K. K. Oehlenschlaeger, E. Frick, M. Glassner, C. Schmid, C. Barner-Kowollik, *Macromol. Rapid Commun.* **2011**, *32*, 807.
[11] T. Pauloehrl, G. Delaittre, V. Winkler, A. Welle, M. Bruns, H. G. Börner, A. M. Greiner, M. Bastmeyer, C. Barner-Kowollik, *Angew. Chem., Int. Ed.* **2012**, *51*, 1071.
[12] C. M. Preuss, T. Tischer, C. Rodriguez-Emmenegger, M. M. Zieger, M. Bruns, A. S. Goldmann, C. Barner-Kowollik, *J. Mater. Chem. B* **2014**, *2*, 36.

[13] T. Tischer, T. K. Claus, M. Bruns, V. Trouillet, K. Linkert, C. Rodriguez-Emmenegger, A. S. Goldmann, S. Perrier, H. G. Börner, C. Barner-Kowollik, *Biomacromolecules* **2013**, *14*, 4340.
[14] M. Glassner, K. K. Oehlenschlaeger, A. Welle, M. Bruns, C. Barner-Kowollik, *Chem. Commun.* **2013**, *49*, 633.
[15] T. Pauloehrl, A. Welle, K. K. Oehlenschlaeger, C. Barner-Kowollik, *Chem. Sci.* **2013**, *4*, 3503.
[16] E. Vedejs, T. H. Eberlein, R. G. Wilde, *J. Org. Chem.* **1988**, *53*, 2220.
[17] J. Chiefari, Y. K. Chong, F. Ercole, J. Krstina, J. Jeffery, T. P. T. Le, R. T. A. Mayadunne, G. F. Meijs, C. L. Moad, G. Moad, E. Rizzardo, S. H. Thang, *Macromolecules* **1998**, *31*, 5559.
[18] G. Moad, E. Rizzardo, S. H. Thang, *Aust. J. Chem.* **2012**, *65*, 985.
[19] G. Moad, E. Rizzardo, S. H. Thang, *Aust. J. Chem.* **2009**, *62*, 1402.
[20] G. Moad, E. Rizzardo, S. H. Thang, *Aust. J. Chem.* **2006**, *59*, 669.
[21] G. Moad, E. Rizzardo, S. H. Thang, *Aust. J. Chem.* **2005**, *58*, 379.
[22] G. Moad, E. Rizzardo, *Macromolecules* **1995**, *28*, 8722.
[23] M. Kato, M. Kamigaito, M. Sawamoto, T. Higashimura, *Macromolecules* **1995**, *28*, 1721.
[24] J.-S. Wang, K. Matyjaszewski, *J. Am. Chem. Soc.* **1995**, *117*, 5614.
[25] M. Kaupp, T. Tischer, A. F. Hirschbiel, A. P. Vogt, U. Geckle, V. Trouillet, T. Hofe, M. H. Stenzel, C. Barner-Kowollik, *Macromolecules* **2013**, *46*, 6858.
[26] M. Winkler, J. O. Mueller, K. K. Oehlenschlaeger, L. Montero de Espinosa, M. A. R. Meier, C. Barner-Kowollik, *Macromolecules* **2012**, *45*, 5012.
[27] L. Nebhani, C. Barner-Kowollik, *Adv. Mater.* **2009**, *21*, 3442.
[28] M. T. Gokmen, F. E. Du Prez, *Prog. Polym. Sci.* **2012**, *37*, 365.
[29] H. Kawaguchi, *Prog. Polym. Sci.* **2000**, *25*, 1171.
[30] M. Slater, M. Snauko, F. Svec, J. M. J. Fréchet, *Anal. Chem.* **2006**, *78*, 4969.
[31] A. R. Vaino, K. D. Janda, *J. Comb. Chem.* **2000**, *2*, 579.
[32] A. P. Vogt, T. Tischer, U. Geckle, A. M. Greiner, V. Trouillet, M. Kaupp, L. Barner, T. Hofe, C. Barner-Kowollik, *Macromol. Rapid Commun.* **2013**, *34*, 916.
[33] R. Barbey, L. Lavanant, D. Paripovic, N. Schüwer, C. Sugnaux, S. Tugulu, H.-A. Klok, *Chem. Rev.* **2009**, *109*, 5437.
[34] A. S. Goldmann, L. Barner, M. Kaupp, A. P. Vogt, C. Barner-Kowollik, *Prog. Polym. Sci.* **2012**, *37*, 975.
[35] M. Kaupp, A. P. Vogt, J. C. Natterodt, V. Trouillet, T. Gruendling, T. Hofe, L. Barner, C. Barner-Kowollik, *Polym. Chem.* **2012**, *3*, 2605.
[36] H. Lee, S. M. Dellatore, W. M. Miller, P. B. Messersmith, *Science* **2007**, *318*, 426.
[37] O. Pop-Georgievski, C. Rodriguez-Emmenegger, A. de los Santos Pereira, V. Proks, E. Brynda, F. Rypacek, *J. Mater. Chem. B* **2013**, *1*, 2859.
[38] O. Pop-Georgievski, S. Popelka, M. Houska, D. Chvostová, V. Proks, F. Rypàček, *Biomacromolecules* **2011**, *12*, 3232.
[39] S. H. Ku, C. B. Park, *Biomaterials* **2010**, *31*, 9431.
[40] J.-L. Wang, K.-F. Ren, H. Chang, F. Jia, B.-C. Li, Y. Ji, J. Ji, *Macromol. Biosci.* **2013**, *13*, 483.
[41] O. Pop-Georgievski, D. Verreault, M. O. Diesner, V. Proks, S. Heissler, F. Rypáček, P. Koelsch, *Langmuir* **2012**, *28*, 14273.
[42] V. Proks, J. Jaroš, O. Pop-Georgievski, J. Kučka, Š. Popelka, P. Dvořák, A. Hampl, F. Rypáček, *Macromol. Biosci.* **2012**, *12*, 1232.
[43] C. M. Preuss, A. S. Goldmann, V. Trouillet, A. Walther, C. Barner-Kowollik, *Macromol. Rapid Commun.* **2013**, *34*, 640.
[44] C. N. LaFratta, J. T. Fourkas, T. Baldacchini, R. A. Farrer, *Angew. Chem., Int. Ed.* **2007**, *46*, 6238.
[45] S. Maruo, J. T. Fourkas, *Laser Photon. Rev.* **2008**, *2*, 100.
[46] M. Malinauskas, M. Farsari, A. Piskarskas, S. Juodkazis, *Phys. Rep.* **2013**, *533*, 1.
[47] T. G. Leong, A. M. Zarafshar, D. H. Gracias, *Small* **2010**, *6*, 792.
[48] A. S. Quick, H. Rothfuss, A. Welle, B. Richter, J. Fischer, M. Wegener, C. Barner-Kowollik, *Adv. Funct. Mater.* **2014**, *24*, 3571.
[49] B. Neises, W. Steglich, *Angew. Chem., Int. Ed.* **1978**, *17*, 522.
[50] T. Gruendling, M. Kaupp, J. P. Blinco, C. Barner-Kowollik, *Macromolecules* **2011**, *44*, 166.
[51] M. Buback, T. Junkers, P. Vana, *Macromol. Rapid Commun.* **2005**, *26*, 796.
[52] C. Boyer, V. Bulmus, P. Priyanto, W. Y. Teoh, R. Amal, T. P. Davis, *J. Mater. Chem.* **2009**, *19*, 111.
[53] L. Nebhani, D. Schmiedl, L. Barner, C. Barner-Kowollik, *Adv. Funct. Mater.* **2010**, *20*, 2010.
[54] A. S. Goldmann, T. Tischer, L. Barner, M. Bruns, C. Barner-Kowollik, *Biomacromolecules* **2011**, *12*, 1137.
[55] M. Bruns, C. Barth, P. Brüner, S. Engin, T. Grehl, C. Howell, P. Koelsch, P. Mack, P. Nagel, V. Trouillet, D. Wedlich, R. G. White, *Surf. Interface Anal.* **2012**, *44*, 909.
[56] E. H. Lock, D. Y. Petrovykh, P. Mack, T. Carney, R. G. White, S. G. Walton, R. F. Fernsler, *Langmuir* **2010**, *26*, 8857.
[57] S. Hansson, V. Trouillet, T. Tischer, A. S. Goldmann, A. Carlmark, C. Barner-Kowollik, E. Malmström, *Biomacromolecules* **2013**, *14*, 64.
[58] O. Pop-Georgievski, N. Neykova, V. Proks, J. Houdkova, E. Ukraintsev, J. Zemek, A. Kromka, F. Rypacek, *Thin Solid Films* **2013**, *543*, 180.
[59] F. Binns, J. A. G. King, S. N. Mishra, A. Percival, N. C. Robson, G. A. Swan, A. Waggott, *J. Chem. Soc. C* **1970**, 2063.
[60] G. A. Swan, in *Fortschritte der Chemie Organischer Naturstoffe / Progress in the Chemistry of Organic Natural Products* Vol. *31* (Eds: W. Herz, H. Grisebach, G. W. Kirby), Springer, Vienna **1974**, p.521.
[61] J. Fischer, J. B. Mueller, J. Kaschke, T. J. A. Wolf, A.-N. Unterreiner, M. Wegener, *Opt. Express* **2013**, *21*, 26244.
[62] C. Strazielle, H. Benoit, O. Vogl, *Eur. Polym. J.* **1978**, *14*, 331.
[63] K. L. Parry, A. G. Shard, R. D. Short, R. White, J. D. Whittle, A. Wright, *Surf. Interface Anal.* **2006**, *38*, 1497.
[64] J. Scofield, *J. Electron Spectrosc. Relat. Phenom.* **1976**, *8*, 129.
[65] S. Tanuma, C. J. Powell, D. R. Penn, *Surf. Interface Anal.* **1994**, *21*, 165.
[66] C. M. Herzinger, B. Johs, W. A. McGahan, J. A. Woollam, W. Paulson, *J. Appl. Phys.* **1998**, *83*, 3323.